Peptide- and Long-Chain Polyamine- Induced Synthesis of Micro- and Nanostructured Titanium Phosphate and Protein Encapsulation

Kathryn E. Cole,[†] Andrea N. Ortiz,[‡] Martin A. Schoonen,[§] and Ann M. Valentine*[,†]

Department of Chemistry, Yale University, New Haven, Connecticut 06511, Department of Chemistry, California State Polytechnic University, Pomona, California 91768, and Department of Geosciences and Center for Environmental Molecular Science, Stony Brook University, Stony Brook, New York 11794-2100

Received April 6, 2006. Revised Manuscript Received May 26, 2006

Poly(allylamine) (a mimic of biopolyamines) and the R5 peptide (a repeat unit of a silaffin protein isolated from a diatom) induce the formation of mineralized titanium from soluble titanium(IV) precursors. These reactions proceed under mild aqueous conditions. Scanning electron microscopy shows that the nanometer to micrometer diameter particles induced by poly(allylamine) are spherical under a range of conditions, while those induced by the R5 peptide include spheres and fused structures. Dynamic light scattering experiments confirm the SEM results and reveal that the particles range in size from 2 nm to 5 μm. The surface charge is negative at neutral pH. Energy dispersive X-ray spectroscopy shows the composition to be primarily titanium, oxygen, and phosphorus. The solids are amorphous at room temperature by powder X-ray diffraction but the material induced by poly(allylamine) converts to cubic crystalline TiP_2O_7 with annealing to 800 °C. Infrared spectroscopy suggests that the biomolecule mineralization inducers are encapsulated in the solid. Discrete poly(allylamine)-induced spheres are formed only between pH 7−9.5, with polydispersity strongly dependent on pH. The surface of the poly(allylamine)-induced spheres becomes smoother at higher reaction temperatures. Green fluorescent protein can be immobilized in the solid induced by poly(allylamine) but not R5 peptide under the conditions examined.

Introduction

Biomineralization, the deposition of inorganic materials by organisms, has been studied for some time.[1,2] The formation of biosilica by diatoms is one well-studied example. These unicellular, photosynthetic organisms are found mostly in marine environments as the major component of phytoplankton.[3] Diatoms precipitate silica for the construction of their cell walls at near neutral pH and under ambient temperatures and pressures. The intricate designs of their cell walls reflect a controlled biosilicification mechanism.

The molecules and mechanisms responsible for diatom biosilicification are active areas of investigation.[4,5] Silaffins are proteins that direct biosilicification in diatoms. They were originally identified in *Cylindrotheca fusiformis*[6] but have since been studied further[7−10] and identified in other diatom species.[11] A 19 amino acid peptide called R5 (H_2N−SSKKSGSYSGSKGSKRRIL−COOH), a repeat unit from the silaffin Sil1 of *C. fusiformis*, mimics some aspects of the silica-precipitating activity of the natural silaffin,[6,12] even in the absence of the phosphorylation and polyamine modifications of the natural protein. The activity of this peptide has been studied in detail[13−15] and used to immobilize proteins in nanostructured silica.[16,17] The latter is of considerable technological interest because it results in active and stabilized immobilized enzymes. Along with the silaffin proteins, polyamines are intimately involved in biosilica formation in diatoms.[18,19] Biomimetic silica precipitation by polyamines including poly(allylamine) (PAA) has been studied in vitro.[20−26]

* To whom correspondence should be addressed. E-mail: ann.valentine@yale.edu.
[†] Yale University.
[‡] California State Polytechnic University.
[§] Stony Brook University.

(1) Lowenstam, H. A.; Weiner, S. *On Biomineralization*; Oxford University Press: New York, 1989.
(2) Mann, S. *Biomineralization: Principles and Concepts in Bioinorganic Materials Chemistry*; Oxford University Press: New York, 2001.
(3) Round, F. E.; Crawford, R. M.; Mann, D. G. *The Diatoms: Biology & Morphology of the Genera*; Cambridge University Press: Cambridge, 1990.
(4) Sumper, M.; Kröger, N. *J. Mater. Chem.* **2004**, *14*, 2059−2065.
(5) Patwardhan, S. V.; Clarson, S. J.; Perry, C. C. *J. Chem. Soc., Chem. Commun.* **2005**, 1113−1121.
(6) Kröger, N.; Deutzmann, R.; Sumper, M. *Science* **1999**, *286*, 1129−1132.
(7) Kröger, N.; Deutzmann, R.; Sumper, M. *J. Biol. Chem.* **2001**, *276*, 26066−26070.
(8) Kröger, N.; Lorenz, S.; Brunner, E.; Sumper, M. *Science* **2002**, *298*, 584−586.
(9) Poulsen, N.; Sumper, M.; Kröger, N. *Proc. Natl. Acad. Sci. U.S.A.* **2003**, *100*, 12075−12080.
(10) Wenzl, S.; Deutzmann, R.; Hett, R.; Hochmuth, E.; Sumper, M. *Angew. Chem., Int. Ed.* **2004**, *43*, 5933−5936.
(11) Poulsen, N.; Kröger, N. *J. Biol. Chem.* **2004**, *279*, 42993−42999.
(12) Brott, L. L.; Naik, R. R.; Pikas, D. J.; Kirkpatrick, S. M.; Tomlin, D. W.; Whitlock, P. W.; Clarson, S. J.; Stone, M. O. *Nature* **2001**, *413*, 291−293.
(13) Naik, R. R.; Whitlock, P. W.; Rodriguez, F.; Brott, L. L.; Glawe, D. D.; Clarson, S. J.; Stone, M. O. *J. Chem. Soc., Chem. Commun.* **2003**, 238−239.
(14) Rodriguez, F.; Glawe, D. D.; Naik, R. R.; Hallinan, K. P.; Stone, M. O. *Biomacromolecules* **2004**, *5*, 261−265.
(15) Knecht, M. R.; Wright, D. W. *J. Chem. Soc., Chem. Commun.* **2003**, 3038−3039.
(16) Luckarift, H. R.; Spain, J. C.; Naik, R. R.; Stone, M. O. *Nat. Biotechnol.* **2004**, *22*, 211−213.
(17) Naik, R. R.; Tomczak, M. M.; Luckarift, H. R.; Spain, J. C.; Stone, M. O. *J. Chem. Soc., Chem. Commun.* **2004**, 1684−1685.
(18) Kröger, N.; Deutzmann, R.; Bergsdorf, C.; Sumper, M. *Proc. Natl. Acad. Sci. U.S.A.* **2000**, *97*, 14133−14138.
(19) Sumper, M.; Brunner, E.; Lehmann, G. *FEBS Lett.* **2005**, *579*, 3765−3769.

10.1021/cm060807b CCC: $33.50 © 2006 American Chemical Society
Published on Web 08/19/2006

Besides silica, diatoms in their natural habitat can contain up to 1254 ppm titanium in their frustules.[27] This value reflects one of the highest titanium concentrations known in biology. The accumulation of titanium in diatom frustules in the photosynthetic zone of the ocean may contribute to the depletion of soluble titanium at the surface.[28] This surface-depleted profile is consistent with scavenging by biotic or abiotic processes. Other studies show that residual titanium in the water decreases during a bloom of diatom growth.[29,30] When cultured in the presence of elevated levels of titanium, diatoms incorporate titanium in their frustules.[31]

In general, the recognized use of titanium minerals by extant organisms is rare and may result from collection of titanium-containing minerals from the environment, rather than "biotitanification."[32−35] Recent research suggests, however, that titanium minerals may have played a role in the origins of life.[36]

The current work addresses three key questions: Could the occurrence of titanium in diatom frustules be due to the titanium-precipitating ability of diatom biomolecules? Put another way: are the diatom biosilicification inducers also chemically competent to precipitate titania (TiO_2) or another titanium material? Can materials of unusual or controllable morphology be prepared by controlling reaction conditions, including the identity of the titanium-containing precursor and the precipitation inducer? Finally, can proteins be encapsulated in biotemplated titanium materials for potential biotechnological applications, as has been demonstrated for silica?

Other recent research has focused on the biomolecule-induced precipitation of titanium minerals. Silica-precipitating proteins (silicateins) from siliceous sponges induce amorphous/nanocrystalline titania to form along the protein filaments when treated with a soluble Ti(IV)-containing precursor.[37] When anchored to a surface, silicatein catalyzes the formation of layered titanium dioxide.[38] When displayed on the surface of an *Escherichia coli* cell in a phosphate-containing buffer, silicatein instead induces the formation of layered titanium phosphates.[39] The latter are of particular interest because titanium phosphates have potential applications in separations and in catalysis and because routes to their synthesis typically involve high-temperature reactions with phosphoric acid. In other recent work, titania was templated by polyethylenimine polymers,[40] by lysine-based low molecular weight gelators,[41] by bacterial cellulose membranes,[42] and by a fungus cell surface[43] to make TiO_2 films, nanotubes, nanowires, and particles.

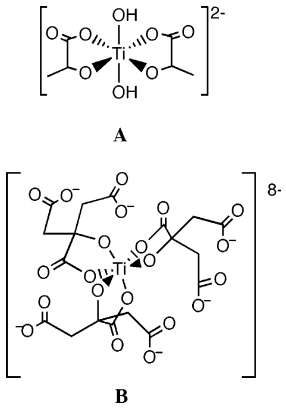

Figure 1. Structures of the complex cations of (A) titanium(IV) bis(ammonium lactato) dihydroxide and (B) titanium(IV) tris(citrate).[51] Complexes shown are the predicted Ti(IV) species near pH 7.

Here we present the rapid formation of micro- and nanostructured mineralized titanium by using a mild aqueous synthesis. Poly(allylamine) (PAA) and the R5 peptide each induce the formation of nanostructured mineralized titanium in vitro from soluble titanium(IV) precursors. Scanning electron microscopy coupled with energy dispersive spectroscopy, X-ray powder diffraction with annealing, Fourier transform infrared spectroscopy, and light scattering are used to image and characterize the particles and bulk materials. The effects of temperature and pH on the particle formation, morphology, and size dispersion are reported. Finally, the immobilization of a green fluorescent protein in the material induced by PAA is detailed.

Materials and Methods

Materials. All aqueous stocks and solutions were prepared with Nanopure-quality water (18.2 MΩ-cm resistivity). Poly(allylamine) (PAA, CAS 30551-89-4) (20 wt % in water, MW ca. 17000) and titanium(IV) bis(ammonium lactato) dihydroxide (Ti−BALDH, CAS 65104-06-5) (50 wt % in water) (Figure 1), both from Aldrich, were used without further purification. A titanium atomic absorption standard (984 ppm) was also from Aldrich. Tiron (4,5-dihydroxy-

(20) Mizutani, T.; Nagase, H.; Fujiwara, N.; Ogoshi, H. *Bull. Chem. Soc. Jpn.* **1998**, *71*, 2017−2022.
(21) Mizutani, T.; Nagase, H.; Ogoshi, H. *Chem. Lett.* **1998**, 133−134.
(22) Sumper, M. *Angew. Chem., Int. Ed.* **2004**, *43*, 2251−2254.
(23) Brunner, E.; Lutz, K.; Sumper, M. *Phys. Chem. Chem. Phys.* **2004**, *6*, 854−857.
(24) Lutz, K.; Groger, C.; Sumper, M.; Brunner, E. *Phys. Chem. Chem. Phys.* **2005**, *7*, 2812−2815.
(25) Belton, D.; Patwardhan, S. V.; Perry, C. C. *Chem. Commun.* **2005**, 3475−3477.
(26) Belton, D. J.; Patwardhan, S. V.; Perry, C. C. *J. Mater. Chem.* **2005**, *15*, 4629−4638.
(27) Martin, J. H.; Knauer, G. A. *Geochim. Cosmochim. Acta* **1973**, *37*, 1639−1653.
(28) Orians, K. J.; Boyle, E.; Bruland, K. W. *Nature* **1990**, *348*, 322−325.
(29) Sholkovitz, E. R.; Price, N. B. *Geochim. Cosmochim. Acta* **1980**, *44*, 163−171.
(30) Skrabal, S. A.; Ullman, W. J.; Luther, G. W. *Mar. Chem.* **1992**, *37*, 83−103.
(31) Riley, J. P.; Roth, I. *J. Mar. Biol. Assn. UK* **1971**, *51*, 63−72.
(32) Stokroos, I.; Litinetsky, L.; van der Want, J. J.; Ishay, J. S. *Nature* **2001**, *411*, 654−655.
(33) Ishay, J. S.; Riabinin, K.; Kozhevnikov, M.; van der Want, H.; Stokroos, I. *Biomacromolecules* **2003**, *4*, 649−56.
(34) Ishay, J. S.; Joseph, Z.; Galushko, D.; Ermakov, N.; Bergman, D. J.; Barkay, Z.; Stokroos, I.; Van der Want, J. *Microsc. Res. Technol.* **2005**, *66*, 259−269.
(35) Cole, K. E.; Valentine, A. M. *Dalton Trans.* **2006**, 430−432.
(36) Senanayake, S. D.; Idriss, H. *Proc. Natl. Acad. Sci. U.S.A.* **2006**, *103*, 1194−1198.
(37) Sumerel, J. L.; Yang, W. J.; Kisailus, D.; Weaver, J. C.; Choi, J. H.; Morse, D. E. *Chem. Mater.* **2003**, *15*, 4804−4809.
(38) Tahir, M. N.; Theato, P.; Muller, W. E. G.; Schroder, H. C.; Borejko, A.; Faiss, S.; Janshoff, A.; Huth, J.; Tremel, W. *Chem. Commun.* **2005**, 5533−5535.
(39) Curnow, P.; Bessette, P. H.; Kisailus, D.; Murr, M. M.; Daugherty, P. S.; Morse, D. E. *J. Am. Chem. Soc.* **2005**, *127*, 15749−15755.
(40) Jia, Q. X.; McCleskey, T. M.; Burrell, A. K.; Lin, Y.; Collis, G. E.; Wang, H.; Li, A. D. Q.; Foltyn, S. R. *Nat. Mater.* **2004**, *3*, 529−532.
(41) Suzuki, M.; Nakajima, Y.; Sato, T.; Shirai, H.; Hanabusa, K. *Chem. Commun.* **2006**, 377−379.
(42) Zhang, D. Y.; Qi, L. M. *Chem. Commun.* **2005**, 2735−2737.
(43) Bansal, V.; Rautaray, D.; Bharde, A.; Ahire, K.; Sanyal, A.; Ahmad, A.; Sastry, M. *J. Mater. Chem.* **2005**, *15*, 2583−2589.

1,3-benzenedisulfonic acid disodium salt), catalase, and butyrylcholinesterase (BChE) were purchased from Sigma. A plasmid encoding a His6-tagged green fluorescent protein (GFP) was a gift from Professor Lynne Regan. The GFP was expressed and purified according to a published procedure.[44] The R5 peptide (H_2N-SSKKSGSYSGSKGSKRRIL$-$COOH) was synthesized and characterized by the W.M. Keck Foundation Biotechnology Resource Facility at Yale University. Titanium(IV) tris(citrate) (Figure 1) was synthesized according to the procedure of Zhou et al.[45]

Precipitation of Titanium-Containing Solids. In a typical reaction with PAA, a 150 μL aliquot of a 2 mM stock solution of PAA (pH 6.8) was added to 375 μL of 0.2 M phosphate buffer (pH 7.4) and 915 μL of dH_2O in a 1.7 mL Eppendorf tube. The combination of PAA and phosphate yields a cloudy microemulsion.[22] The mineralization reaction was initiated by the addition of 60 μL of a 1 M stock solution of Ti$-$BALDH for a total volume of 1.5 mL, yielding final concentrations of 40 mM Ti and 0.2 mM PAA in 50 mM phosphate buffer (pH 7.4). Similar procedures are reported for the precipitation of silica.[13,16,17,22] Reactions employing the less soluble titanium tris(citrate) were identical to those with Ti$-$BALDH, except that 60 μL of 200 mM titanium tris(citrate) was added to induce the reaction, resulting in a final Ti concentration of 8 mM.

For precipitation induced by the R5 peptide, a peptide stock solution was prepared by dissolving peptide in 0.2 M phosphate buffer (pH 7.4.) This combination does not result in an apparent emulsion, as in the case of PAA. The R5 peptide concentration was determined by UV/vis ($\epsilon = 1280\ M^{-1}\ cm^{-1}$). Peptide stock solutions were used within 2 days of preparation. To initiate precipitation, 10 μL of a 1 M stock solution of Ti$-$BALDH was added to approximately 500 nmol of peptide from the stock solution, yielding a typical final volume of 1.5 mL.

Reactions aiming for GFP immobilization employed all final reagent concentrations as described above in addition to GFP at a final concentration of 0.5 μM. For attempted immobilization of catalase and BChE, protein concentrations ranged from 0.03 to 2 μM.

In each case, precipitation occurred immediately upon addition of the titanium precursor to the reaction mixture. Reactions were mixed on a rotary mixer for at least 10 min. In control reactions, each titanium precursor was added in the absence of PAA or peptide; after >1 day only slight precipitation was observed. In other control reactions, carbonate and Tris buffers were used in place of phosphate buffers at the same concentration and pH. Addition of extra titanium precursor to the supernatant or to the solid did not result in further precipitation.

For variable pH studies, 1 M HCl or 1 M NaOH was used to adjust the initial pH of the phosphate buffer and water solutions. The pH was recorded again after the addition of PAA; the pH values reported are those recorded after this addition. Precipitation was induced with the titanium precursor as described above. For variable temperature studies, all reagents were equilibrated to the desired temperature before mixing. After mixing, the reaction mixture was maintained at the specified temperature for approximately 5$-$10 min.

Typically, samples were collected by centrifugation in a microcentrifuge and resuspended in dH_2O before analysis. Particles were resuspended in water and centrifuged to pellet the solid material. This washing procedure was repeated up to 10 times.

Quantitation of Residual Titanium in Supernatant. The supernatant after the precipitation reaction was analyzed for residual titanium by using a spectrophotometric analytical assay.[46,47] A modified procedure using the method of standard additions was employed. Final solutions (1 mL total volume) contained 0.4% Tiron, between 0 and 32 μM Ti from a titanium atomic absorption standard, and 10 μL of supernatant solution in 1.5 M sodium acetate buffer (pH ~5.2). All samples were allowed to equilibrate for at least 30 min prior to measurement at 380 nm.

Scanning Electron Microscopy/Energy Dispersive Spectroscopy. Scanning electron microscopy (SEM) was performed on an FEI XL-30-ESEM-FEG instrument at 10$-$20 kV in either low-vacuum (0.7$-$0.8 Torr) or high-vacuum mode ($<8 \times 10^{-6}$ Torr). Elemental distribution was determined by energy dispersive spectroscopy (EDS) analysis. A thin carbon sputter coating was required for high vacuum. Carbon tape and/or a carbon-2-propanol solution (Ted Pella, Inc.) was used to coat the aluminum sample mount before addition of the sample. Data were analyzed by using the software ImageJ (http://rsb.info.nih.gov/ij/).

Light Scattering and Zeta Potential. Dynamic light scattering was measured on a ZetaPlus - Zeta Potential Analyzer (Brookhaven Instruments Corporation, Stony Brook University). A diluted 2 mL suspension of particles (~500 mg/L of sample diluted in 15 mL of 10 mM KCl) was used. The zeta potentials of the particles were determined with the same instrument by using Phase Angle Light Analysis.[48] All samples were prepared under a laminar flow hood to prevent contamination from dust.

Powder X-ray Diffraction. Samples were analyzed on a Bruker-AXS D8 Focus diffractometer with Cu radiation at 1.54439 Å. Samples were scanned over a range of 10.000° to 80.000° with a step of 0.050° in a $\theta-2\theta$ locked couple scan.

Annealing Studies. The solid was collected by centrifugation and washed at least three times to remove any coprecipitated soluble salts and then was dried under vacuum to remove excess water. The sample was heated in an annealing oven (Laboratory Glass Blowing Inc., Model # 300) in a borosilicate (for 200, 400, or 600 °C) or quartz (800 °C) vial to the required temperature in air. Powder X-ray diffraction was used to assess the crystallinity of the samples after heating to each temperature.

Infrared Spectroscopy. Solid samples, dried under vacuum, were analyzed as Nujol mulls on a Nicolet 6700 Fourier transform infrared spectrometer (FT-IR) using the Transmission ESP Program. Typical experiments averaged 128 scans.

Material Dissolution. Titanium-containing solids were solubilized by using a procedure originally described for freshly precipitated hydrolyzed titanium acid, by using a basic solution of catechol[49] to produce a Ti(IV) tris(catechol) complex.[50]

Results and Discussion

Ti Precursors. Complexes of the Lewis acidic, hydrolysis-prone Ti(IV) are often unstable in aqueous solutions near neutral pH. Titanium(IV) bis(ammonium lactato) dihydroxide (Ti$-$BALDH) and titanium(IV) tris(citrate) (Figure 1) are stable precursors in such solutions. The speciation and properties of titanium tris(citrate) were characterized recently.[51,52] Although the speciation of the Ti$-$BALDH remains uncharacterized, it is available in concentrated solution and was used successfully in recent work,[37$-$39] and

(44) Merkel, J. S.; Regan, L. *J. Biol. Chem.* **2000**, *275*, 29200$-$29206.
(45) Zhou, Z.-H.; Deng, Y.-F.; Jiang, Y.-Q.; Wan, H.-L.; Ng, S.-W. *J. Chem. Soc., Dalton Trans.* **2003**, 2636$-$2638.
(46) Yoe, J. H.; Armstrong, A. R. *Science* **1945**, *102*, 207.
(47) Yoe, J. H.; Armstrong, A. R. *Anal. Chem.* **1947**, *19*, 100$-$102.
(48) Miller, J. F.; Schatzel, K.; Vincent, B. *J. Colloid Interface Sci.* **1991**, *143*, 532$-$554.
(49) Rosenheim, A.; Sorge, O. *Chem. Ber.* **1920**, *53*, 932$-$939.
(50) Borgias, B. A.; Cooper, S. R.; Koh, Y. B.; Raymond, K. N. *Inorg. Chem.* **1984**, *23*, 1009$-$1016.

thus is employed here. In our hands, the Ti−BALDH is more prone to hydrolysis than the Ti tris(citrate), but no quantitative study has been done. When either titanium precursor is incubated in phosphate buffer in the absence of PAA or R5 peptide, only a slight precipitate is observed after an extended time (>1 day). The resulting solid exhibits no interesting micro- or nanostructure (Figure S1, Supporting Information).[37,39]

Precipitant Molecules and Characterization by Microscopy. Poly(allylamine) and the R5 peptide are each effective promoters for the rapid precipitation of mineralized titanium from either titanium tris(citrate) or Ti−BALDH. This induction of precipitation is not a general property of biopolymers. Adding the titanium precursors to other proteins[53] or other amines (data not shown) does not induce the similar rapid formation of solid material.

Addition of Ti tris(citrate) as the titanium precursor to PAA yields a material that exhibits some regions of fused spheres (Figure S2A, Supporting Information), but more frequently displays no such structure (Figure S2B, Supporting Information). Experiments at a range of temperatures fail to yield reproducibly nano- or microstructured material. Light-scattering experiments on the bulk material (see below) are problematic because the sample gels prior to analysis. The Ti tris(citrate) cannot be dissolved to as high a concentration as the Ti−BALDH, and the former complex is more stable to hydrolysis (see above). Taken together, these properties make the Ti tris(citrate) a less favorable starting material for the production of mineralized titanium than the Ti−BALDH. The remainder of the experiments described thus employ Ti−BALDH as a titanium source.

The reaction of Ti−BALDH with PAA at pH 7.4 forms primarily well-defined, polydisperse spheres as observed by using SEM (Figure 2A). Image analysis reveals that the spheres range from 120 nm to 14 μm in diameter and average 2.5 ± 1.6 μm (average of 846 individual measurements on >10 different samples). The R5 peptide induces structures comprised of both spheres (Figure 2B) and fused spheres. Image analysis reveals that the spheres range from 700 nm to 10.6 μm in diameter and average 3.2 ± 1.5 μm (average of 174 individual measurements on >5 different samples). Replacing the phosphate buffer with carbonate or Tris buffer results in unstructured solid material (data not shown). Analysis by using a tiron complexation assay of residual titanium in the supernatant before and after precipitation reveals that at least 50% of the titanium is incorporated in the precipitate under the conditions employed, and addition of more titanium to either the supernatant or the solid does not result in further precipitation.

EDS reveals that the materials produced from Ti−BALDH and PAA or the R5 peptide are composed primarily of titanium, oxygen, and phosphorus (Figure 3) with varying amounts of sodium and chloride. The relative amounts of sodium and chloride vary from sample to sample, most likely

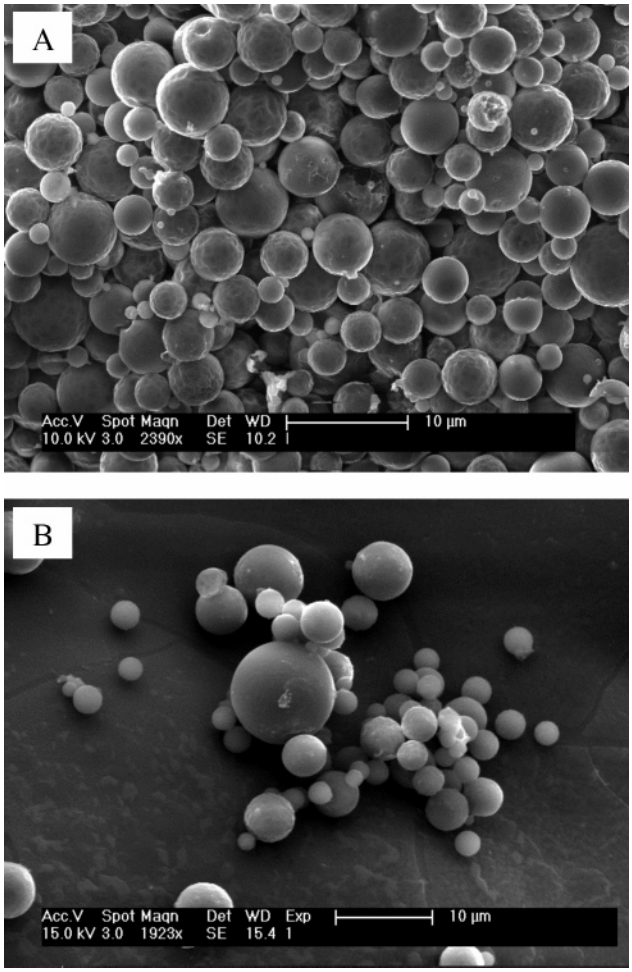

Figure 2. Scanning electron micrographs of titanium-containing spheres induced by treating Ti−BALDH with (A) poly(allylamine) and (B) R5 peptide.

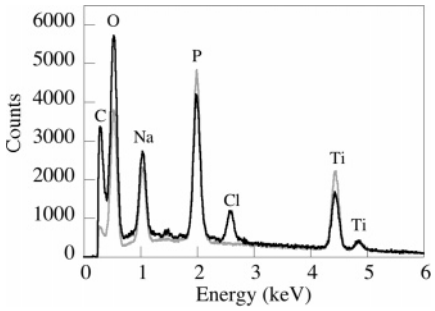

Figure 3. Representative EDS spectra of spheres induced by poly(allylamine) (black) and R5 peptide (gray).

correlating with the amount of sodium phosphate or sodium chloride coprecipitated in the sample (see below). Phosphorus is always present in high concentration and is not removed by washing. Carbon peaks could result from the carbon coating on the sample and sample mount, or from coprecipitated PAA or peptide.

X-ray Diffraction and Annealing. The materials induced from Ti−BALDH with PAA (Figure 4) or peptide (data not shown) at 25 °C and pH 7 are X-ray amorphous at room temperature. That the material is X-ray amorphous does not preclude the formation of locally crystalline regions, but like the diatom frustules themselves, the current materials are amorphous in bulk. The initially white solid induced by PAA

(51) Collins, J. M.; Uppal, R.; Incarvito, C. D.; Valentine, A. M. *Inorg. Chem.* **2005**, *44*, 3431−3440.
(52) Uppal, R.; Incarvito, C. D.; Lakshmi, K. V.; Valentine, A. M. *Inorg. Chem.* **2005**, *45*, 1795−1804.
(53) Tinoco, A. D.; Valentine, A. M. *J. Am. Chem. Soc.* **2005**, *127*, 11218−11219.

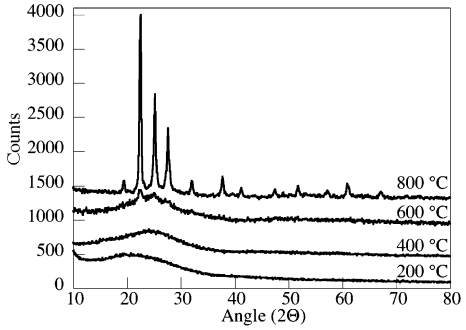

Figure 4. X-ray powder patterns of nanostructured titanium phosphate induced by PAA after annealing to increasing temperature. Spectra were offset by 400 counts for 400 °C annealing, 800 counts for 600 °C annealing, and 1200 counts for 800 °C annealing.

turned yellowish after heating to 200 °C, turned black after heating to 400 °C, and returned to a bright white solid after heating to 800 °C. X-ray powder diffraction reveals the appearance of peaks after annealing to 800 °C, representative of cubic crystalline titanium phosphate TiP_2O_7 (Figure 4) (Joint Committee for Powder Diffraction Studies, Powder Diffraction File #38-1468). This result is similar to the one obtained for titanium phosphate induced by cell-surface-bound silicatein,[39] except that we see no evidence for an intermediate sodium titanium phosphate phase.

Although the molecular mechanism for biomolecule-induced titanium phosphate formation has not been determined, it may be related to that described for silica particle precipitation.[4,13,23] In the case of PAA, the negatively charged phosphate ions interact with the positively charged PAA by electrostatic interactions and/or hydrogen bonding. Several studies of PAA ionization suggest that the polymer amines are mostly protonated below pH 6, and mostly deprotonated above pH 11 in aqueous solution, with an average pK_a around 8.8,[54] although other studies report lower pK_a values (Figure S3, Supporting Information).[55] This interaction between phosphates and amines forms a microscopic phase separation, which can be observed as an emulsion on the macroscopic scale after mixing PAA and phosphate. When the silica precursor is introduced, it dissolves into and/or adsorbs onto the emulsion, forming a "liquid precipitate," which then hardens, producing the particles. The presence of phosphate in the current work, then, may result from this emulsion that coprecipitates with the particles. The multiple Lys and Arg residues in the R5 peptide may behave similarly to the polyamine and afford an analogous mechanism, albeit over a lesser biopolymer length and at different pH values (Figure S3, Supporting Information). The mechanism of the activity of this peptide for silica precipitation has been studied in detail.[13−15] At pH 7, as described above, no emulsion is visible after combining the R5 peptide with phosphate. The suggestion that amines are important moieties for biomineralization is supported by the essentiality of the RRIL motif for biomimetic silicification.[15] Recent work shows that the morphology of silica can be directed by choice of polylysine.[56]

Dynamic Light Scattering. Dynamic light scattering can be used to complement the data obtained by analysis of the SEM images to determine the size of the particles formed at neutral pH. In this way, the entire bulk sample can be analyzed. Measurements of material formed from PAA and Ti−BALDH at 25 °C reveal two predominant scatterer populations centered at approximately 450 nm and 9 μm (Figure S4, Supporting Information). With consideration of the SEM data, which do not show a significant population of particles as large as 9 μm, the larger may be attributed to some clustering. After sonication in a bath for 5−10 min, two populations are found, now centered at 420 nm and 1 μm. Thus, the 450 nm particles are little affected by the sonication treatment, while the micrometer-sized clusters are broken up into smaller particles. Filtration of the sonicated sample through a 5 μm filter removes the micrometer-sized particles scattering most of the light and reveals two additional populations centered at 40 and 170 nm. Thus, the particles produced from poly(allylamine) and Ti−BALDH are polydisperse and range in size from 40 nm to 1 μm, with some larger clusters. This conclusion is in good agreement with SEM investigations of the samples.

The light scattering by material formed using the R5 peptide is more difficult to interpret because the particles are more often fused than those formed using PAA. Initial measurements find scatterers centered at 2 nm and 1.3 μm (Figure S4, Supporting Information). Sonication produces two new populations at 13 and 890 nm. Filtration through a 5 μm filter reveals populations at 40 and 200 nm. In contrast to the populations found from PAA, the sizes determined for particles produced from the R5 peptide do not consistently decrease with sonication and filtration. This result is attributed to the fact that the particles are fused, resulting in a less uniform sample. Also, the larger structures scatter light more than smaller particles do, making a small population of nanoscale particles more difficult to detect. This interpretation of the bulk behavior is in good agreement with the SEM observations.

Zeta potential and mobility measure the effective surface charge of particles as a function of pH. The zeta potential of all particles formed from Ti−BALDH and either PAA or R5 peptide is negative at neutral pH. Measurements on PAA-induced material averaged −2.39 (μ/s)/(V/cm) mean mobility. The material produced by using the R5 peptide was similar, with −2.41 (μ/s)/(V/cm) mean mobility.

Infrared Spectroscopy. IR spectra provide evidence for the incorporation of the PAA and R5 peptide in the precipitated material. The samples were washed extensively before measurement. The materials induced by PAA and by the R5 peptide exhibit peaks that are distinct from one another and that are not present in a control sample (Figure S5, Supporting Information). Compared with Ti−BALDH hydrolyzed by added base in the absence of inducer, the IR spectrum of PAA-induced solid shows a broad absorbance near 3400 cm^{-1} as well as distinct peaks between 1550 and 1650 cm^{-1}. These peaks are characteristic of primary amines. The material induced by R5 peptide instead has features at 880−895, 1630−1695, and 3020−3100 cm^{-1}, which are

(54) Choi, J.; Rubner, M. F. *Macromolecules* **2005**, *38*, 116−124.
(55) Suh, J.; Paik, H. J.; Hwang, B. K. *Bioorg. Chem.* **1994**, *22*, 318−327.
(56) Patwardhan, S. V.; Maheshwari, R.; Mukherjee, N.; Kiick, K. L.; Clarson, S. J. *Biomacromolecules* **2006**, *7*, 491−497.

characteristic of C−H and C═O stretches and a broad feature near 3400 cm^{-1}. These data suggest that the biomolecules are becoming encapsulated in the solids formed as the titanium phosphate precipitates around them. In agreement with this interpretation, addition of more Ti−BALDH to the separated supernatant after solid formation, the pH of which is unchanged, does not result in further precipitation.

Reaction Conditions: Temperature and pH. In an attempt to change the rate of precipitation and encourage more defined monodisperse particles, reactions were conducted using PAA and Ti−BALDH at different temperatures. Precipitation occurs immediately upon adding the titanium precursor in all cases. The SEM images of the variable temperature experiments show that the particles remain unchanged in size and polydispersity (Figure S6, Supporting Information). EDS data suggests that the elemental composition of the particles is the same at the various temperatures. The only clear difference involved the surface smoothness of the particles. Reactions at lower temperature (4 and 25 °C) produce particles with clearly layered and textured surfaces, while those performed at higher temperatures (60 and 80 °C) form particles with smoother surfaces. These results are analogous to work that shows a change in silica surface smoothness as a function of pH,[57] whereas in the current case, changes in pH have a still more dramatic effect.

Variable pH studies on the reaction of PAA with Ti−BALDH reveal that the nano- and microscale morphology is strongly dependent upon the pH of the reaction (Figure 5). Well-defined spheres are only formed between pH 7 and pH 9.5. The slightly basic pH of the ocean environment falls within this limit. Over this range, the amines of the PAA polymer are deprotonated (see above),[54] with concomitant changes in the reactivity of the polymer. In addition, the phosphate buffer (pK_2 of phosphoric acid = 7.2) changes composition over this range (Figure S3, Supporting Information). The pH-dependent interactions of phosphate with polyamines have been studied for their importance to silica precipitation and particle size and that analysis is relevant to the current case.[24] In that work, the authors showed by dynamic light scattering and other techniques that the interaction between the positively charged polyamine and the negatively charged phosphate was strongly dependent on the pH. Both charges decrease with increasing pH, and phase separation and aggregation occurs only at intermediate pH values similar to those observed here. In the current case, a visible emulsion after mixing PAA and phosphate buffer occurs only between pH 7 and pH 9.5, these pH values correlating with the formation of disperse spheres. Below pH 7 and above pH 10, no such emulsion forms, or else it forms and then redissolves quickly. The hydrolysis rate of Ti−BALDH likely increases with increasing pH. Taken together, these factors result in unstructured solid being formed below pH 7 and above pH 9.5. SEM reveals that the spheres formed at pH 9.5 (1.7 ± 0.9 μm) are more monodisperse than those observed at pH 7 (2.5 ± 1.6 μm). The ∼100 nm diameter nanospheres contributing to the small extreme of the range of sphere sizes at pH 7 are not observed at pH 9.5, and most of the spheres correspond instead to the 1−2 μm populations observed by both SEM and light scattering.

The pH dependence along with the requirement for phosphate supports the idea that dibasic phosphate associates with partially protonated **(**bio**)**polymer (either polyamine or peptide), providing a template for mineralization. The material appears to be deposited in a layered fashion, perhaps around the immobilized precipitating biomolecule. Many room-temperature samples exhibit a surface with evident layers. One of the clearest depictions of this phenomenon is shown as Figure 6. In this case as in many, apparent "seams" bisect the spheres in the outermost layer in spheres of a range of sizes.

Protein Immobilization. Active and stabilized catalase and butyrylcholinesterase (BChE) have been immobilized in silica nanoparticles precipitated by the R5 peptide.[13,16,17] Immobilized protein was evidenced by the expected protein bands in Coomassie-stained SDS-PAGE gels after dissolution of the solid. Relatively mild conditions liberated the enzymes from the silica. Enzyme activity measurements in the solid confirmed that active enzyme was encapsulated.

Addition of catalase or BChE to titanium mineralization reactions did not change the morphology or elemental composition of the materials according to SEM and EDS. SDS-PAGE analysis of the supernatant after precipitation revealed that most (>90%) of the protein remained in solution. In this case, liberation and detection of potentially small amounts of encapsulated enzymes is more difficult than for silica. Heating in mild base does not resdissolve the solid. More vigorous heating in a basic catechol solution[49] successfully redissolves the amorphous titanium phosphate. In control experiments with proteins, however, the higher temperature and basic conditions used in this method result in protein degradation. The sensitivity of the enzymes to the dissolution conditions means that small amounts of immobilized enzyme would not be reliably detected. Attempts to detect enzyme activity in the particles by the spectrophotometric assays used for catalase and BChE[13,16,17] were foiled by light scattering by the particles. Protein size is an additional concern. Catalase is a tetramer of ∼60 kD subunits. Its structure shows that the complex is 10.5×5 nm,[58] which is not much smaller than the smallest particles. Similarly, BChE is a tetramer of 65.1 kD subunits.

Because of the difficulties in detecting small amounts of these immobilized enzymes, attention turned to the green fluorescent protein (GFP) as an easily detectable proof-of-principle case, where detection of immobilization would depend neither on SDS-PAGE of protein from a dissolved solid nor on an enzymatic activity assay, but could be easily ascertained by the green fluorescence of the solid.[59] In addition, GFP is smaller than either catalase or BChE. The construct used here is a 29 kD monomeric protein approximately 4.2 nm long × 2.4 nm wide.[60]

(57) Patwardhan, S. V.; Clarson, S. J. *Mater. Sci. Eng. C* **2003**, *23*, 495−499.

(58) Fita, I.; Rossmann, M. G. *Proc. Natl. Acad. Sci. U.S.A.* **1985**, *82*, 1604−1608.

(59) Roth, K. M.; Zhou, Y.; Yang, W. J.; Morse, D. E. *J. Am. Chem. Soc.* **2005**, *127*, 325−330.

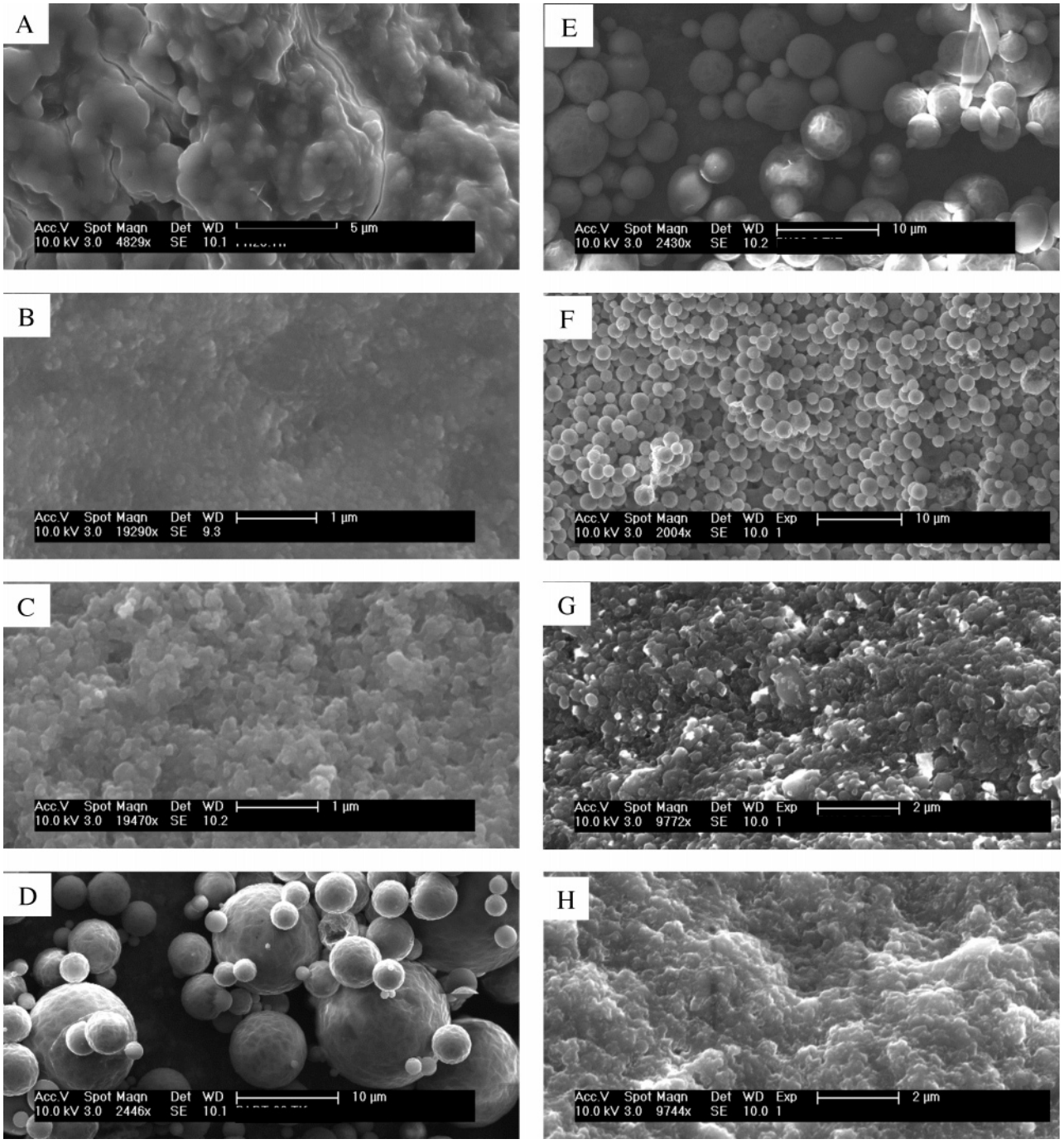

Figure 5. Titanium phosphate materials formed from poly(allylamine) and Ti−BALDH at room temperature at different pH values: (A) pH 2, (B) pH 4.6, (C) pH 5.4, (D) pH 7.0, (E) pH 8.9, (F) pH 9.5, (G) pH 10, and (H) pH 10.7.

The mineralization reaction induced by PAA but not the R5 peptide results in GFP immobilization in the solid at pH 7. Figure 7 shows the solids formed after addition of Ti−BALDH, as well as the supernatant solutions from several washes of those solids. In Figure 7A, for PAA, the majority of the GFP is immobilized in the solid, while a small amount remains in the supernatant after precipitation. SDS-PAGE of the supernatant after mineralization reveals that ~95% of the 0.5 μM GFP is immobilized in the PAA-precipitated reaction. The protein is not removed from the solid by repeated washing, even in the presence of 0.5 M imidazole. The PAA-induced particles appear similar by SEM to those formed in the absence of GFP (Figure S7, Supporting Information). In control reactions, incubation of GFP with PAA in the absence of Ti−BALDH, or with Ti−BALDH in the absence of PAA, do not result in any precipitation. Incubation of freshly precipitated titanium phosphate material with GFP does not result in protein adsorption. This result suggests strongly that the GFP is encapsulated in the solid during precipitation and is not simply tightly associated with the surface. Dissolution of the solid,[49] which clearly contains GFP, fails to yield a band corresponding to GFP by SDS-PAGE, and control experi-

(60) Brejc, K.; Sixma, T. K.; Kitts, P. A.; Kain, S. R.; Tsien, R. Y.; Ormo, M.; Remington, S. J. *Proc. Natl. Acad. Sci. U.S.A.* **1997**, *94*, 2306−2311.

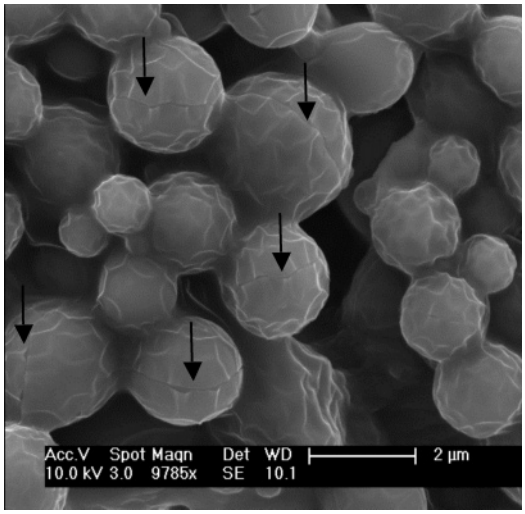

Figure 6. Titanium phosphate spheres formed by PAA and Ti−BALDH at 25 °C, pH 7. The layered, faceted structure, as well as the seam separating each sphere into hemispheres, is visible.

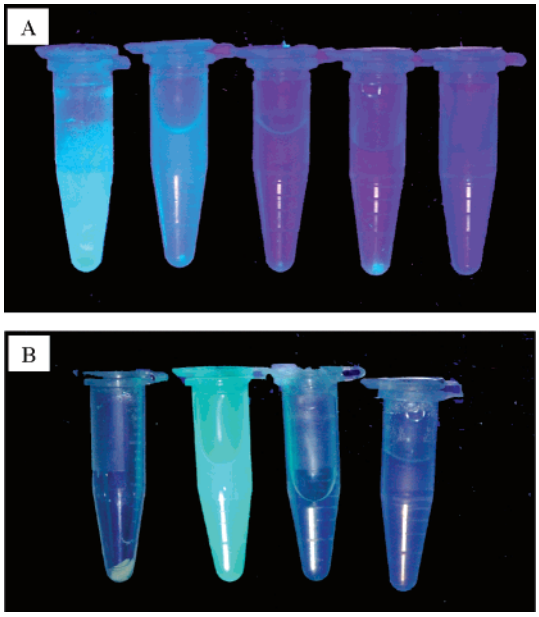

Figure 7. Protein encapsulation as detected by irradiation at 365 nm. (A) Left to right: Encapuslated GFP in titanium phosphate induced by PAA; supernatant after precipitation; wash 1 (water, 1 mL); wash 2 (water, 1 mL); wash 3 (500 mM imidazole, 1 mL). (B) Left to right: Mineralized titanium showing no significant protein encapsulation induced by the R5 peptide; supernatant from precipitation; wash 1; wash 2.

ments confirm that GFP does not survive the dissolution conditions. These results agree with those described above for catalase and BChE.

The solid induced by R5 peptide contains only negligible GFP, as shown in Figure 7B. The solid produced is not visibly green under irradiation at 365 nm, and the supernatant after precipitation contains >95% of the GFP protein by SDS-PAGE.

Taken together, these results suggest that GFP is immobilized in the titanium phosphate spheres induced by PAA but not the R5 peptide. The preference for immobilization with PAA but not R5 is still under investigation. One possibility is that PAA may offer more sites of positive charge to the negatively charged GFP (pI 5.622) as compared to the R5 peptide (Figure S3, Supporting Information). These favorable electrostatic interactions may then promote protein encapsulation. Alternatively, the emulsion observed for the PAA but not the R5 peptide in the presence of phosphate may facilitate protein immobilization.

Conclusion

In conclusion, poly(allylamine), a mimic of long-chain biopolyamines, and the R5 peptide, a repeat unit of a silaffin isolated from diatoms, effectively promote the formation of micro- and nanostructured mineralized titanium in vitro from two different soluble and stable titanium-containing precursors in the presence of phosphate. This result suggests that the natural biomolecules modeled by these polymers are chemically competent to induce "biotitanification," which may be responsible for the occurrence of titanium in diatom frustules and for the surface depletion of soluble titanium from natural waters. The materials induced by PAA and the R5 peptide are similar in elemental composition, consisting mainly of titanium, oxygen, and phosphorus, but differ in some important respects. Those formed using PAA with the Ti−BALDH precursor are well-defined spheres ranging from ∼40 nm to ∼10 μm in diameter, with the surface characteristics and particle size controllable by experimental conditions including temperature and pH. Solids induced using R5 peptide are spheres and fused spheres. XRD indicates that they are X-ray amorphous at room temperature, but annealing the sample to >800 °C results in a crystalline phase of TiP_2O_7. Particles induced by either PAA or the R5 peptide precipitate immediately on the lab time scale and the surface charge of the resulting material is negative at neutral pH. Only the PAA, however, has thus far afforded immobilized protein in the mineralized titanium phosphate.

Note Added in Proof. While this paper was in press, a report appeared describing synthesis of titanium dioxide by using the R5 peptide. Ref: Sewell, S. L.; Wright, D. W. *Chem. Mater.* **2006**, *18*, 3108−3113.

Acknowledgment. We thank Professor Lynne Regan for the gift of plasmid encoding the GFP, Mr. F. Marc Michel for assistance with the JCPDS-PDF database, Dr. Zhenting Jiang for help with SEM and EDS, Mr. Daryl C. Smith for help with high-temperature annealing, and Dr. Christopher Incarvito for assistance with powder XRD. We thank Mr. Arthur Tinoco for synthesis and characterization of titanium tris(citrate) and help with the tiron assay. Peptide synthesis was performed at the W. M. Keck Foundation Biotechnology Research Laboratory at Yale University. Light scattering facilities at Stony Brook University are maintained with support from NSF-Chemistry through the Center for Environmental Molecular Science. K.E.C. was supported by a National Institutes of Health Predoctoral Traineeship in Biophysical Chemistry (GM08283). A.N.O. was supported by the Science, Technology and Research Scholars (STARS) Program, which is funded by the Howard Hughes Medical Institute and Boehringer-Ingelheim Pharmaceutical, Inc. We also thank the Yale University Department of Chemistry for support.

Supporting Information Available: SEM images, pH-dependent speciation plots, DLS data, and FTIR data. This material is available free of charge via the Internet at http://pubs.acs.org.

CM060807B